2017

Field Characterization of Field Capacity and Root Zone Available Water Capacity for Variable Rate Irrigation

Tsz Him Lo
University of Nebraska-Lincoln, tszhimlo@huskers.unl.edu

Derek M. Heeren
University of Nebraska-Lincoln, derek.heeren@unl.edu

Luciano Mateos
Instituto de Agricultura Sostenible

Joe D. Luck
University of Nebraska-Lincoln, jluck2@unl.edu

Derrel L. Martin
University of Nebraska-Lincoln, derrel.martin@unl.edu

See next page for additional authors

FIELD CHARACTERIZATION OF FIELD CAPACITY AND ROOT ZONE AVAILABLE WATER CAPACITY FOR VARIABLE RATE IRRIGATION

T. Lo, D. M. Heeren, L. Mateos, J. D. Luck, D. L. Martin, K. A. Miller, J. B. Barker, T. M. Shaver

ABSTRACT. *Accurate spatial characterization of field capacity (FC) and root zone available water capacity (R) can enhance site-specific management practices—such as variable rate irrigation—to lower input costs, reduce contaminant leaching, and/or improve crop yield. Measuring the volumetric water content after wet soils drain following substantial precipitation can provide a field estimate of FC. The average FC (FC_a) for the managed root zone was determined at thirty-two locations in a topographically variable field in south central Nebraska. The difference between FC and permanent wilting point estimates—computed using a pedotransfer function—yielded values for R for the observation locations. Sampling locations were too sparse for reliable interpolation across the field. Therefore, relationships between a surrogate, or predictor, variable and soil water properties were used to provide spatial distributions of FC and R for the field. Field estimates of FC_a and R were more strongly correlated to elevation (correlation coefficient, r = -0.77 and -0.76, respectively) than to deep soil apparent electrical conductivity (r = -0.46 and -0.39, respectively). Comparing maps of FC_a and R from gSSURGO to maps from field characterization yielded a root mean squared difference of 0.031 m^3 m^{-3} for FC_a and 34 mm for R. Sampling seven locations across the elevation range in this field produced FC_a and R prediction functions that achieved 95% and 87%, respectively, of the reduction in the standard error achievable with a larger number of sampling locations. Spatial characterization of FC_a and R depends on identifying a suitable predictor variable(s) based on field knowledge and available spatial data. Well-chosen variables may allow satisfactory predictions using several sampling locations that are distributed over the entire field. Ultimately, the costs and benefits of spatial characterization should be considered when evaluating site-specific water management.*

Keywords. *Available water capacity, Electrical conductivity, Field capacity, Permanent wilting point, Spatial variability, Variable rate irrigation.*

Conventional center-pivot irrigation (CI) does not involve site-specific water applications; rather, growers seek to apply a uniform depth throughout the field, accepting that portions of the field may receive more or less water than ideal. The emerging technology of variable rate irrigation (VRI) enables growers "to spatially vary water application depths to address specific soil, crop, and/or other conditions" (Evans et al., 2013). The technology is well-developed (Kranz et al., 2012) and commercially available; however, research on management practices for VRI lacks equivalent advancement (Hedley et al., 2009; McCarthy et al., 2014; Daccache et al., 2015; O'Shaughnessy et al., 2016; and Stone et al., 2016). Improving spatial characterization of soil properties remains a critical need.

Tailoring VRI to site-specific conditions creates benefits when conditions vary within a field. VRI can reduce pumpage compared to CI without sacrificing yield by setting spatially variable thresholds for initiating irrigation (Ritchie and Amato, 1990). Lo et al. (2016) analyzed potential pumpage reduction by estimating the difference in undepleted available soil water at the end of the growing season. Using VRI to mine undepleted water in regions of a field with larger available water capacity (AWC, definitions of selected terms are in the Appendix) could reduce pumpage by 25 mm y^{-1} or more for 13% of the center-pivot fields in Nebraska compared to well-managed CI. Other benefits include reduced deep percolation and fertilizer leaching (Sadler et al., 2000). Adoption of VRI may be most advantageous when yield quality and/or quantity are sensitive to over-irrigation—such as for cotton

Submitted for review in June 2016 as manuscript number NRES 11963; approved for publication by the Natural Resources & Environmental Systems Community of ASABE in June 2017.

The authors are **Tsz Him Lo, ASABE Member,** Graduate Research Assistant, **Derek M. Heeren, ASABE Member,** Assistant Professor and Robert B. Daugherty Water for Food Global Institute Faculty Fellow, Department of Biological Systems Engineering, University of Nebraska, Lincoln, Nebraska; **Luciano Mateos,** Research Scientist and Robert B. Daugherty Water for Food Global Institute Global Fellow, Instituto de Agricultura Sostenible, CSIC, Córdoba, Spain; **Joe D. Luck, ASABE Member,** Associate Professor, **Derrel L. Martin, ASABE Fellow,** Professor and Robert B. Daugherty Water for Food Global Institute Faculty Fellow, **Keith A. Miller, former** Graduate Research Assistant, **J. Burdette Barker, Post-Doctoral Research Associate**, Department of Biological Systems Engineering, University of Nebraska, Lincoln, Nebraska; and **Tim M. Shaver**, Associate Professor, West Central Research and Extension Center, University of Nebraska–Lincoln, North Platte, Nebraska. **Corresponding author:** Derek M. Heeren, 241 L. W. Chase Hall, Lincoln, NE 68583-0726; phone: 402-472-8577; e-mail: derek.heeren@unl.edu.

(Grimes et al., 1969), wine grape (Matthews and Anderson, 1988), and soybeans (Brady et al., 1974). Additionally, VRI may alleviate yield losses from waterlogged soil due to increased denitrification or other nutrient losses (UNL Extension, 2014), lack of aeration (Kanwar et al., 1988), and/or inability to operate farm machinery (Sadler et al., 2005).

Managing VRI systems requires a method to determine irrigation timing and application amounts to specific management zones—essentially irrigation scheduling for each tract. Two common methods of scientific irrigation scheduling rely on the knowledge of soil water properties. One method calculates soil water depletion as the difference between current soil water content and field capacity (FC) within the managed root zone, i.e., the soil depth considered for irrigation management. Irrigation commences when the depletion equals the sum of the net irrigation depth and the local rainfall allowance. The second method calculates soil water depletion fraction, first subtracting permanent wilting point (WP) from current soil water content within the managed root zone and then dividing by root zone available water capacity. Irrigation starts when the soil water depletion fraction reaches management allowed depletion (MAD; Merriam, 1966), which is generally selected to be smaller than the depletion fractions that cause plant water stress (Sadras and Milroy, 1996; Allen et al., 1998; Steduto et al., 2009). If one of these irrigation scheduling methods is adopted in each VRI management zone to optimize the application depths over that zone, the distribution of FC or *R* across the field would need to be known.

In other words, capturing VRI benefits requires accurate spatial data. The required accuracy may exceed the level available in gSSURGO soil surveys (NRCS, 2015). Delineation of soils into discrete soil map units in soil surveys occurred at a scale not intended for precision agriculture (Brevik et al., 2003) and was not georeferenced using Global Positioning System (GPS) receivers. Furthermore, soil properties in surveys originated from representative locations, which rarely aligned with a specific soil polygon. Therefore, surveys do not account for natural or manmade differences in the FC and *R* data between sampling locations and the point of interest. Previous research utilized a two-step procedure where FC and *R* were first determined at multiple field locations and were then predicted throughout the field using a predictor variable (Hezarjaribi and Sourell, 2007; Jiang et al., 2007). Following this procedure to map site-specific FC and *R* may be more appropriate than using gSSURGO for in-season management and in-depth analyses of the economic advantages of VRI.

The challenge becomes determination of FC and R throughout the field. A standard method for estimating WP has been the pressure plate with 1500 kPa of tension (Romano and Santini, 2002). At the same time, the volumetric water content at -1500 kPa (θ_{1500}) has been found to be relatively well-predicted from soil composition data through pedotransfer functions (PTFs; Saxton and Rawls, 2006). Some site-specific studies have used the pressure plate method (Hezarjaribi and Sourell, 2007; Jiang et al., 2007; Hedley and Yule, 2009), whereas others have used PTFs (King et al., 2006; Haghverdi et al., 2015).

Determining FC is more challenging. Although the soil water potential associated with FC (ψ_{FC}) is somewhat related to texture, it is difficult to predict (Romano and Santini, 2002). Uncertainty results from the characteristics of each soil horizon and the interactions between horizons. For example, ψ_{FC} and thus FC can increase with soil layering (Martin et al., 1990; Romano and Santini, 2002). Soil water contents vary widely between soil textures in the range of soil water potentials where ψ_{FC} may occur; thus, accurate estimates of FC can be problematic. Determining FC for an intact soil profile captures *in-situ* effects of free drainage. The classic experiment for measuring FC involves saturating the soil profile, covering the soil surface, and monitoring soil water content and drainage (Romano and Santini, 2002). King et al., (2006) used this method for VRI research; however, it is impractical for irrigation managers. A less demanding method for determining FC would be to measure "observational field capacity" (FC_{obs}), an estimate of FC determined in the field but under non-experimental conditions. The concept of FC_{obs} is consistent with the suggestion by Martin et al. (1990) that "[a] good indication of the field capacity water content can be determined by sampling field soils one to three days after a thorough irrigation or rain and when crop water use is small." Also, FC_{obs} has been measured in previous site-specific research (Hezarjaribi and Sourell, 2007; Jiang et al., 2007; Haghverdi et al., 2015). A value of *R* calculated from FC_{obs} and WP can be referred to as "observational *R*" (R_{obs}). Despite the benefits of using FC_{obs} compared to other methods of determining FC, few studies have quantified the spatial variability in FC_{obs} or R_{obs} for VRI management (Hezarjaribi and Sourell, 2007; Jiang et al., 2007).

Once FC_{obs} and R_{obs} have been determined at multiple sampling locations, one must forecast parameter values for unsampled location within the field. Unless the sampling locations are dense, interpolation based on spatial autocorrelation alone may poorly predict FC_{obs} and R_{obs} at points far from sampling points. Predictor variables strongly correlated to FC_{obs} or R_{obs} that can be measured densely with less effort than FC_{obs} or R_{obs} are often employed to predict the spatial distribution of FC_{obs} or R_{obs}. A commonly used predictor variable is apparent soil electrical conductivity (EC_a). In theory, EC_a is a function of the volume of the solid phase, the volume of the liquid phase in fine pores, the electrical conductivity of the solid phase, and the electrical conductivity of the liquid phase in large pores (Rhoades et al., 1989). Researchers have used regression (Hezarjaribi and Sourell, 2007; Jiang et al., 2007; Hedley and Yule, 2009), geostatistics, and machine learning (Haghverdi et al., 2015) to predict the spatial distribution of FC and *R* from EC_a. We will use the term "field characterization" to represent the procedure of determining FC or *R* from *in-situ* measurements (i.e., FC_{obs} or R_{obs}) at multiple sampling locations and then predicting throughout the field using predictor variables.

Our goal was to develop methods to characterize FC_{obs} and R_{obs} within a field. Multiple spatially dense properties

were evaluated for predictor variables for a field in south central Nebraska. Then, FC_{obs} and R_{obs} maps produced by field characterization were compared with soil survey maps. Finally, sampling at two to ten locations were simulated to design sampling schemes and estimate the accuracy of spatial predictions of FC_{obs} and R_{obs}. The best variables for predicting FC_{obs} and R_{obs} and the resultant accuracy may be specific to the sampled field; however, the procedure should be generalizable to a wide range of fields.

METHODS

FIELD SITE

The study was conducted on a 26-ha center-pivot-irrigated field located in Hamilton County, Nebraska (latitude: 40.832°, longitude: -98.015°). The soils are classified as Hastings silt loam and silty clay loam (Fine smectitic, mesic Udic Argiustolls) with a small area of Hobbs silt loam (Fine-silty, mixed, superactive, nonacid, mesic Mollic Ustifluvents) in the southwest corner of the field. The highest elevation occurred in the northern area of the field and the land slopes downward into two valleys in the south (fig. 1). The difference between the maximum and minimum elevation was 12 m (USGS, 2014). The National Hydrography Dataset (Simley and Carswell, 2009) indicates that each valley contained an ephemeral stream. The valley in the southwest portion of the field contained an eroded channel. The channel was dry at the beginning of the 2014 growing season, but remained inundated for much of the year. The channel and its banks were uncropped and inhabited by riparian vegetation (fig. 1; FSA, 2014). The valley in the eastern portion of the field did not form a distinct channel. The soil surface showed signs of overland flow, but ponded water was not observed during the 2014 growing season.

Measurement locations were selected along topographic transects to characterize the hydrological variability (fig. 1). Measurement locations were concentrated within two hillslope segments where the slope varied the most. Nine slope positions were monitored along a pair of longer transects extending south into the wider valley. Seven slope positions were monitored along a pair of shorter transects extending east into the narrower valley. The ridge-tilled crop rows were oriented in a north-south direction. The transects aligned with crop rows were referred to as the parallel transects, whereas the transects orthogonal to crop rows were referred to as the perpendicular transects. The parallel transects spanned a larger elevation range but contained gentler slopes than the perpendicular transects (fig. 2).

SOIL SAMPLING AND SOIL MOISTURE MEASUREMENT

On 3 and 9 June 2014, a hydraulic probe (Giddings Machine Company, Windsor, Colo.) was used to extract soil cores and install aluminum neutron gauge access tubes at measurement locations. Soil samples—centered at depths of 0.15, 0.46, 0.76, 1.07, 1.37, and 1.68 m below the soil surface—were extracted from the cores. Samples were assumed to represent the 0.30-m layer centered at the specified depth. Samples were trimmed to a length of approximately 0.10 m. Actual lengths were measured and samples were oven-dried to determine the bulk density and volumetric water content (θ_v). Ward Laboratories, Inc. (Kearney, NE) ascertained the textural composition and organic matter content of each sample. Cores at the 0.15-m depth were unavailable at two locations. Soil properties at the missing locations were assumed to match values at corresponding positions on the paired transects.

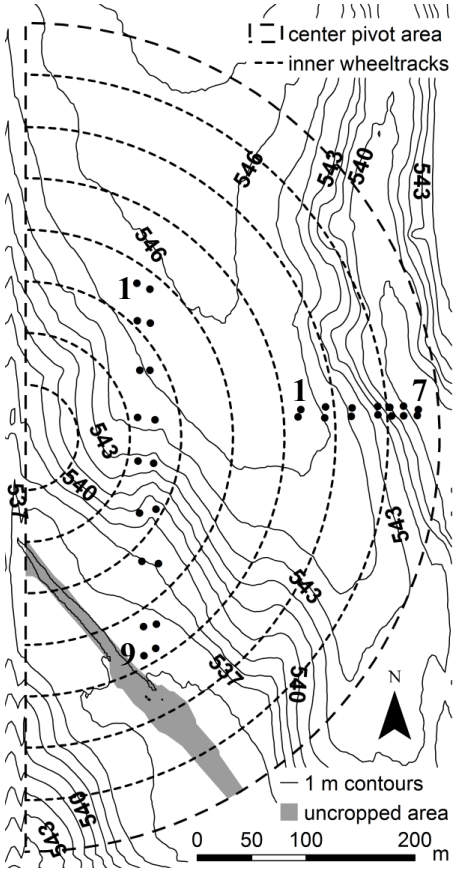

Figure 1. Topographic map of the field site. Measurement locations (dots) form a pair of transects parallel to crop rows (north-south) and perpendicular to crop rows. Highest and lowest positions on transects are numbered. Elevations are in meters above mean sea level.

Soil moisture was measured with a neutron gauge (503 Elite Hydroprobe, CPN International, Concord, Calif.). Measurements were centered at the same depths as for soil sampling. Measurements were 30 s in duration and were assumed to represent the 0.30-m layer centered at the measurement depth. Neutron gauge readings were taken when tubes were installed. A standard count—taken in the shielded position for 256 s— was used to compute count ratios. Count ratios were compared with the θ_v values of the soil samples (fig. 3). Samples whose shape or bulk density was suspect were omitted from consideration. The linear regression between count ratio and θ_v represents the field-specific neutron gauge calibration. A separate calibration was used for the 0.15-m depth. Neutron readings on subsequent days were transformed into count ratios using a standard count for the respective day. The linear calibration was used to compute θ_v.

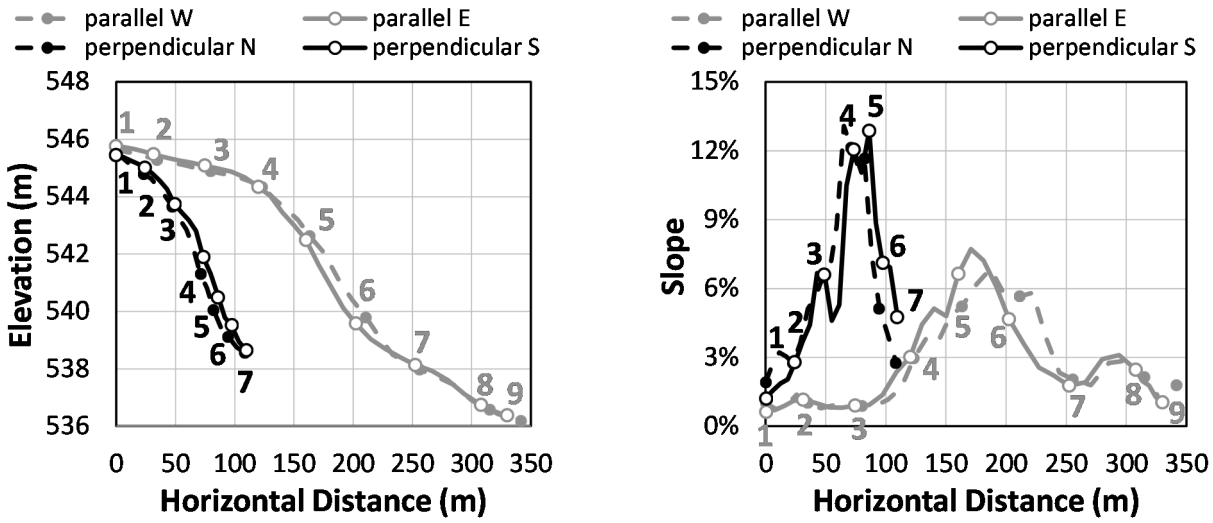

Figure 2. Elevation and slope along transects parallel and perpendicular to crop rows versus horizontal distance from the top of each transect. The 32 measurement locations are marked by dots and labeled with their respective slope position number.

POINT DETERMINATION OF $FC_{OBS,A}$, WP, AND R_{OBS}

The antecedent precipitation from 1 October 2013 to 17 June 2014 was 452 mm, which was slightly above average (NCEI, 2017). The FC_{obs} was determined from neutron probe readings on 18 June 2014, which was three days after a 25-mm rain in the area (NDNR, 2017). The precipitation was sufficient to replenishing the 1.22-m managed root zone to FC. This assessment is supported by increases in θ_v at the 1.37-m and 1.68-m depths following access tube installation 15 and 12 days earlier. Unlike classic experiments for measuring FC, the managed root zone was not recently saturated, and drainage rates were not confirmed to be negligible. However, θ_v on 18 June 2014 was expected to serve as a sufficiently accurate *in-situ* estimate of FC (FC_{obs}). The average FC_{obs} ($FC_{obs,a}$) across the managed root zone was calculated by averaging FC_{obs} at the 0.15-, 0.46-, 0.76-, and 1.07-m depths.

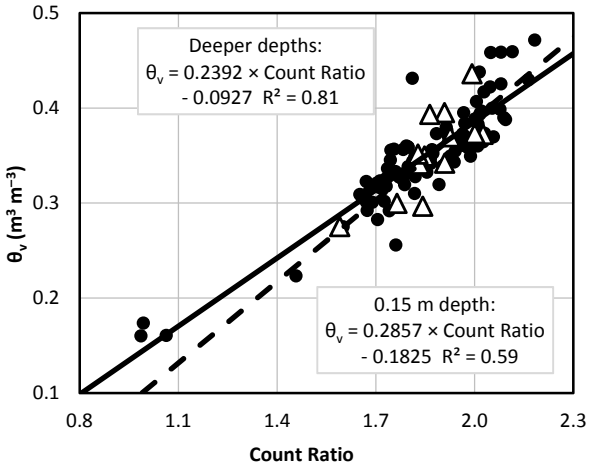

Figure 3. Field-specific calibrations of volumetric water content (θ_v) vs. soil to standard count ratio for neutron gauge. Calibrations are for the 0.15-m measurement depth (triangles, dashed line, and bottom equation) and for deeper measurement depths (0.46, 0.76, 1.07, 1.37, and 1.68 m; circles, solid line, and top equation).

The Saxton and Rawls (2006) pedotransfer function was used to estimate the WP for specific layers and locations. This PTF has been commonly used for Nebraska (Deck, 2010; Mortensen, 2011; Rudnick and Irmak, 2014). The WP value was estimated by entering a tension of 1500 kPa into the PTF. Other inputs included the sand content, clay content, bulk density and organic matter content. The average WP (WP_a) across the managed root zone was calculated by averaging WP at the 0.15-, 0.46-, 0.76-, and 1.07-m depths.

Observational available water capacity (AWC_{obs}) was calculated by subtracting predicted WP from FC_{obs}. The average AWC_{obs} ($AWC_{obs,a}$) across the managed root zone was calculated by averaging AWC_{obs} at 0.15-, 0.46-, 0.76-, and 1.07-m depths. Observational root zone available water capacity (R_{obs}) was the product of $AWC_{obs,a}$ and the managed root zone depth of 1.22 m.

SPATIAL DATASETS

The gridded Soil Survey Geographic (gSSURGO) 10-m soil map unit raster for Nebraska (NRCS, 2015) and the 1/9 arc-second (about 3 m) National Elevation Dataset (NED) digital elevation model (DEM) tile that encompassed the field (USGS, 2014) were obtained. In gSSURGO, soil map units include one or more components, each representing a fraction of the area for that map unit. In turn, each component is comprised of one or more soil horizons. Each horizon represents a specified thickness within a soil profile for that horizon. Values of R and average FC (FC_a) for a 1.22-m managed root zone were calculated for each component using the gSSURGO tabular data. Then, R and FC_a for each map unit were calculated by weighting component values by the percent composition of that component.

Apparent soil electrical conductivity (EC_a) was measured throughout the field using a georeferenced on-the-go electrode-type sensor system (MSP, Veris Technologies, Salina, Kan.) on 23 April 2015. With 24 mm of rain during the previous seven days (NDNR, 2017), the soil was moist. Anhydrous ammonia at 247 kg ha^{-1} of N was applied

uniformly on 30 March 2015, which was 24 days before EC sampling (23 April 2015). The EC_a sensor system travelled along north-south passes (parallel with crop row direction) that were spaced approximately 30-m apart. An EC_a sampling point was omitted if a shallow EC_a reading was beyond 1.5 interquartile ranges from the first and third quartiles of all shallow EC_a readings, or if a deep EC_a reading was beyond 1.5 interquartile ranges from the first and third quartiles of all deep EC_a readings. Interpolation between EC_a data points was performed using ordinary kriging, as implemented in Geostatistical Wizard of ArcGIS 10.2 (ArcGIS, 2013). A shallow EC_a raster and a deep EC_a raster were produced, each with the same cell size as the DEM. An EC_a ratio (Kitchen et al., 2005) raster was computed using Raster Calculator in ArcGIS by dividing the value of each shallow EC_a raster cell by the value of the corresponding deep EC_a raster cell.

The coordinates of the FC_{obs} and R_{obs} measurement locations were obtained using a handheld GPS device (GPSMAP 64s, Garmin, Olathe, Kan.). Each measurement location was assigned the value of the elevation, shallow EC_a, deep EC_a, and EC_a ratio of the raster cell encompassing the measurement location.

Spatial Prediction and Sampling Schemes

A regression equation between relative elevation (height above the minimum elevation) and $FC_{obs,a}$, along with a second function for R_{obs}, was generated for the measurement locations. A piecewise approach was adopted to avoid extrapolation beyond the range of elevations at the measurement locations. Specifically, points above the highest measurement location were assigned the values of $FC_{obs,a}$ and R_{obs} computed from the regression equations with the highest measurement location. Likewise, points below the lowest measurement location were assigned the value of $FC_{obs,a}$ and R_{obs} from the regression equations using the lowest measurement location. The piecewise functions were applied to the DEM using Raster Calculator in ArcGIS to produce $FC_{obs,a}$ and R_{obs} maps.

The effect of the number of sampling locations (n) on the accuracy of the piecewise functions for $FC_{obs,a}$ and R_{obs} was analyzed through simulation. Locations along the western parallel transect or the northern perpendicular transect constituted the calibration set. Locations along the parallel east transect or the perpendicular south transect formed the validation set. For each $n \in (2, 4, 6, 10)$, one sampling scheme was simulated, which sampled n locations from the calibration set. For each $n \in (3, 5, 7, 8, 9)$, two sampling schemes were simulated, each sampling n locations from the calibration set. Sampling schemes incorporated the elevation range of the calibration set while prioritizing coverage of intermediate elevations. The measurement locations at the highest and lowest elevations were sampled in all schemes.

For each scheme, piecewise functions for $FC_{obs,a}$ and R_{obs}—like those based on all measurement locations—were constructed from sampled locations. A balance between matching higher-order trends and the risk of overfitting was desired. The polynomial order of the regression equations was limited to one for sampling schemes with $n = 2$, to $(n - 2)$ for sampling schemes with $2 < n < 6$, and to 3 for sampling schemes with $n \geq 6$. Similarly, the polynomial order for R_{obs} was one for sampling schemes with $n = 2$, to $(n - 2)$ for sampling schemes with $2 < n < 7$, and 4 for sampling schemes with $n \geq 7$. The standard error of the estimate (s) for each piecewise function was calculated for the validation set. All regression parameters were estimated from the calibration set; thus the degrees of freedom were equal to the number of measurement locations in the validation set.

A three-parameter equation represented the relationship between s and n (eq. 1). The strength of the relationship between $FC_{obs,a}$ or R_{obs} and the predictor variable (relative elevation) was denoted s_∞, which was the asymptotic value of s as n approaches infinity. The magnitude of spatial variability for $FC_{obs,a}$ or R_{obs} was described by s_1, the value of s at $n = 1$. The complexity of the relationship between $FC_{obs,a}$ or R_{obs} and predictor variable(s) was described by k, the exponential decay coefficient.

$$s = s_\infty + \left(s_1 - s_\infty\right) e^{-k(n-1)} \quad (1)$$

The parameter s_1 was the value of s for the mean value of the calibration set relative to the validation set. The parameter s_∞ was the value of s for the whole calibration set when applied to the validation set. The parameter k was determined using the Solver add-in in Microsoft Excel (2010) after the observed values of s for $FC_{obs,a}$ or R_{obs} were averaged among sampling schemes with equal n. For a given n, the percentage of the maximum achievable reduction in the value of s was calculated as $(s_1 - s) / (s_1 - s_\infty)$. All statistical computations were conducted in Microsoft Excel.

Results and Discussion

Spatial Variability of Soil Water Properties

The variability of soil water properties along the parallel and perpendicular transects was evaluated to ascertain the effect of slope position. Property values for the pair of observations at the same slope position were averaged and plotted against the slope position (fig. 4). Recall from figure 2 that smaller slope positions represent the hilltops, middle positions the hillside and larger slope positions the toe of the hill. Slopes were steepest for the middle positions and were steeper for the perpendicular transect than the parallel transect.

The FC_{obs} appeared to change where the hillslope transformed from convex to concave (figs. 4a-b). At the 0.46-m depth, FC_{obs} decreased along the convex slopes (parallel slope positions 1-5 and perpendicular slope positions 1-4) and increased along the concave portion (parallel slope positions 6-9 and perpendicular slope positions 5-7). At 0.76 and 1.07 m, FC_{obs} was relatively low along the convex part (parallel slope positions 1-5 and perpendicular slope positions 1-3) and relatively high along the concave portion (parallel slope positions 6-9 and perpendicular slope positions 5-7). No consistent relationship in FC_{obs} at 0.15 m to slope position was observed. The biggest differences in FC_{obs} among the

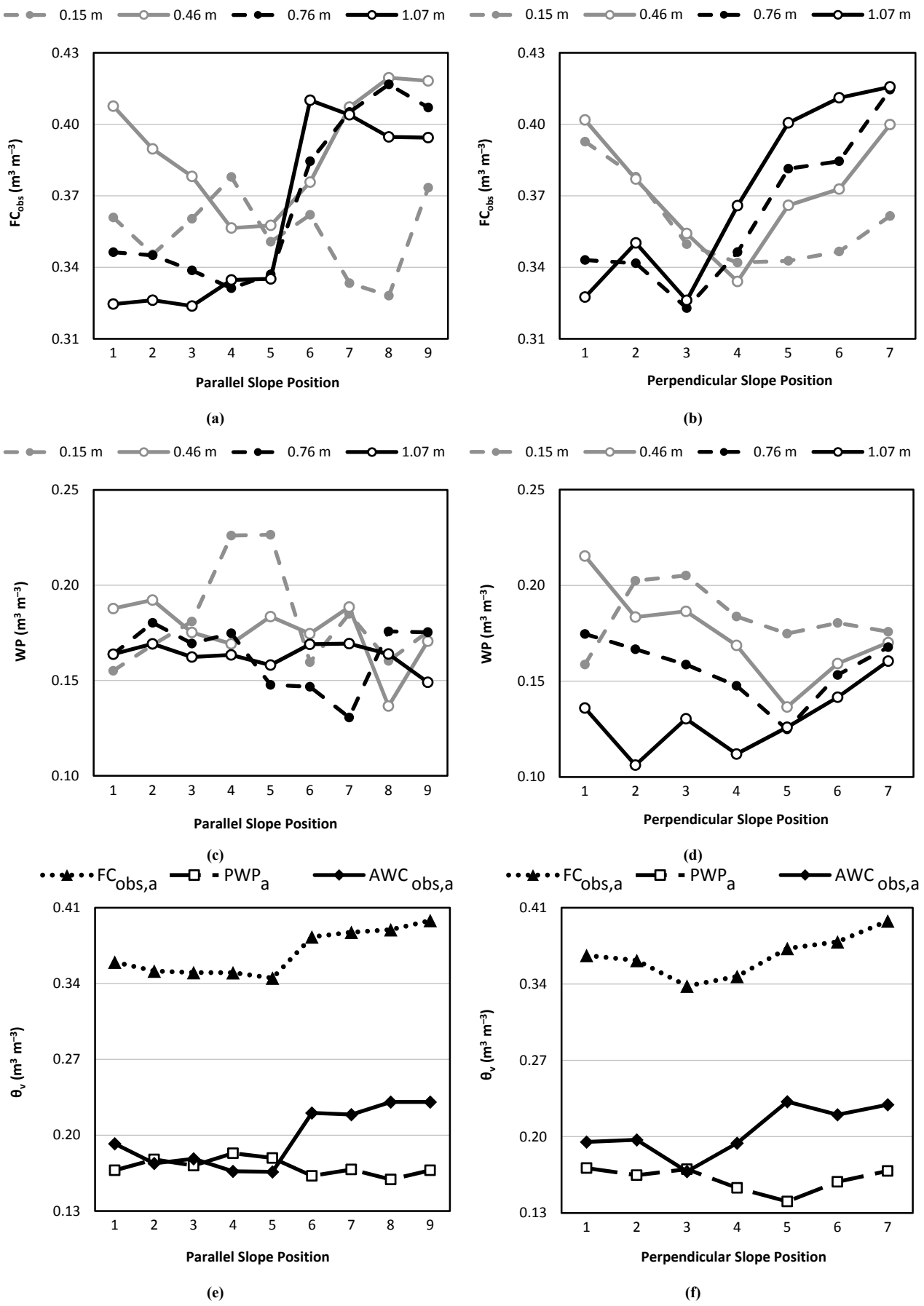

Figure 4. Observational field capacity (FC_{obs}) (a-b), permanent wilting point (WP) estimated by pedotransfer function (c-d), and FC_{obs}, WP, and observational available water capacity ($FC_{obs,a}$, WP_a, and $AWC_{obs,a}$) averaged over the 1.22-m managed root zone (e-f) at four soil depths.

measurement locations occurred at the 0.76- and 1.07-m depths, with ranges of 0.08 to 0.09 m^3 m^{-3}.

Two trends in WP were observed along the two pairs of topographic transects (figs. 4c-d). At the 0.15 m depth, WP was higher along the shoulder of the slopes (parallel slope positions 4-5 and perpendicular slope positions 2-3) than elsewhere. At 0.76 m, WP was lower along the backslopes (parallel slope positions 5-7 and perpendicular slope positions 4-6) than elsewhere. The largest differences in WP among measurement locations did not consistently occur in any one of the four measurement depths within the managed root zone.

The average value of FC_{obs}, WP, and AWC_{obs} over the 1.22-m managed root zone was determined (figs. 4e-f). The $FC_{obs,a}$ decreased slightly along the convex slopes, rose sharply along the transition portion, and increased slightly along the concave section. No consistent spatial pattern in WP_a was observed along either transect. The $AWC_{obs,a}$ was lower along the convex part of the slopes and higher along the concave portions.

Distribution of Apparent Electrical Conductivity

Apparent electrical conductivity has been used to infer soil properties in many studies. We mapped EC_a to determine how well it related to soil water properties. The shallow EC_a was lowest near the hilltops and in the bottom of the wider valley in the southwest region. Values were moderate along east-facing slopes of the narrower valley in the east, and high along south-facing slopes of the wider valley (fig. 5a). Deep EC_a was low in the bottom of the wider valley, high in the southeastern portion of the field, and moderate elsewhere (fig. 5b). The EC_a ratio was low on hilltops, moderate along east-facing slopes of the narrower valley, and high along south-facing slopes in the wider valley (fig. 5c).

Predictor Variables

Since it was impractical to measure soil water properties across an entire field, we sought a surrogate parameter that relates well to soil water properties, i.e., a predictor variable. Two spatially dense variables that we considered were the EC_a and elevation. The range of EC_a variables along the parallel transects was larger than for the perpendicular transects, yet the range of $FC_{obs,a}$ and R_{obs} are similar (fig. 6). The $FC_{obs,a}$ and R_{obs} were moderately well correlated with shallow (results not shown) and deep EC_a (r = -0.62 for $FC_{obs,a}$ and r = -0.60 for R_{obs}) for the parallel transects (figs. 6a and 6c). However, both shallow and deep EC_a were not correlated to $FC_{obs,a}$ or R_{obs} at the 0.05 statistical significance level for the perpendicular transects (figs. 6a and 6c). The EC_a ratio was not correlated to $FC_{obs,a}$ or R_{obs} at the 0.05 statistical significance level for either pair of transects. Smoothing the EC_a maps would not improve correlation because the spatial trends of EC_a did not match the spatial trends in FC_{obs} and R_{obs}. The relationship between EC_a and $FC_{obs,a}$ or R_{obs} was overall poor or inconsistent between transects; thus, none of the EC_a variables were a suitable predictor variable of $FC_{obs,a}$ and R_{obs} at this field site.

In contrast, $FC_{obs,a}$ and R_{obs} were strongly negatively correlated with elevation for parallel transects and moderately negatively correlated with elevation for perpendicular transects (figs. 6b and 6d). Both field capacity and available water capacity were higher at the toe of the hill, decreased along the hillslope and then increased somewhat near the top of the hill. Values near the hilltop were consistently smaller than at the toe of the hill. This

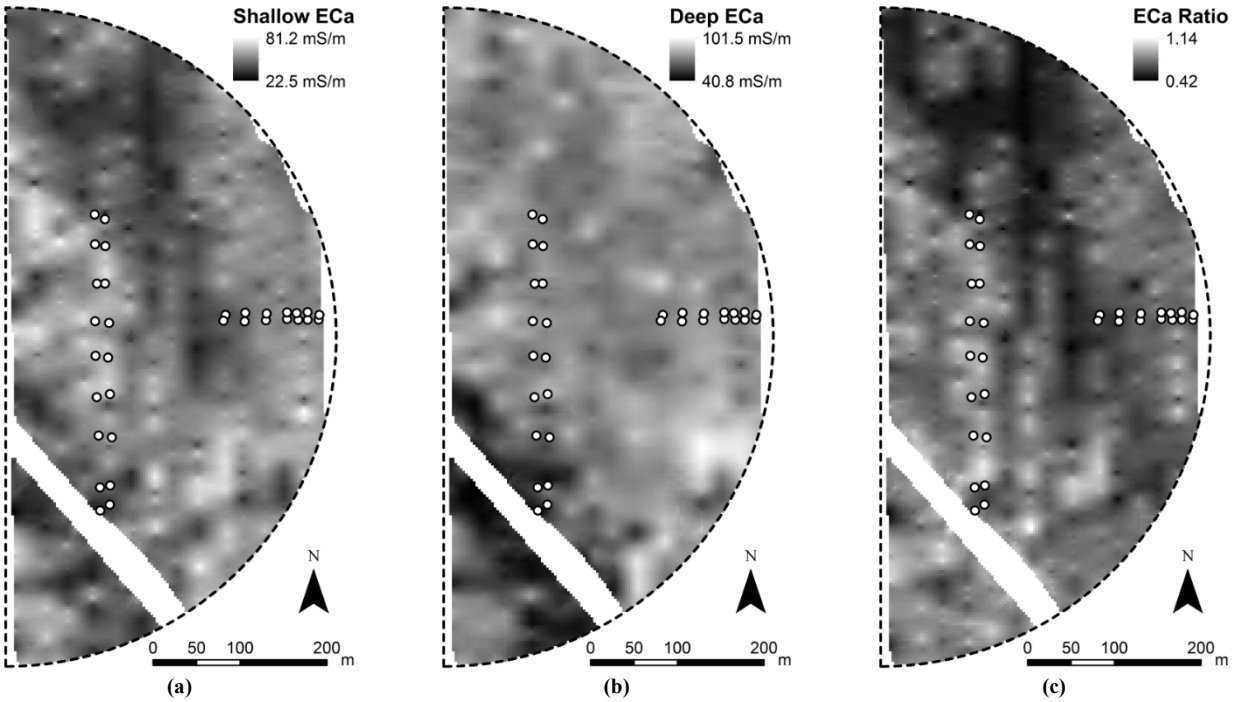

Figure 5. Kriged maps of (a) shallow apparent soil electrical conductivity (EC_a), (b) deep EC_a, and (c) the ratio of shallow EC_a to deep EC_a, as measured by an on-the-go electrode-type sensor system. Measurement locations for FC_{obs} and R_{obs} were indicated as dots.

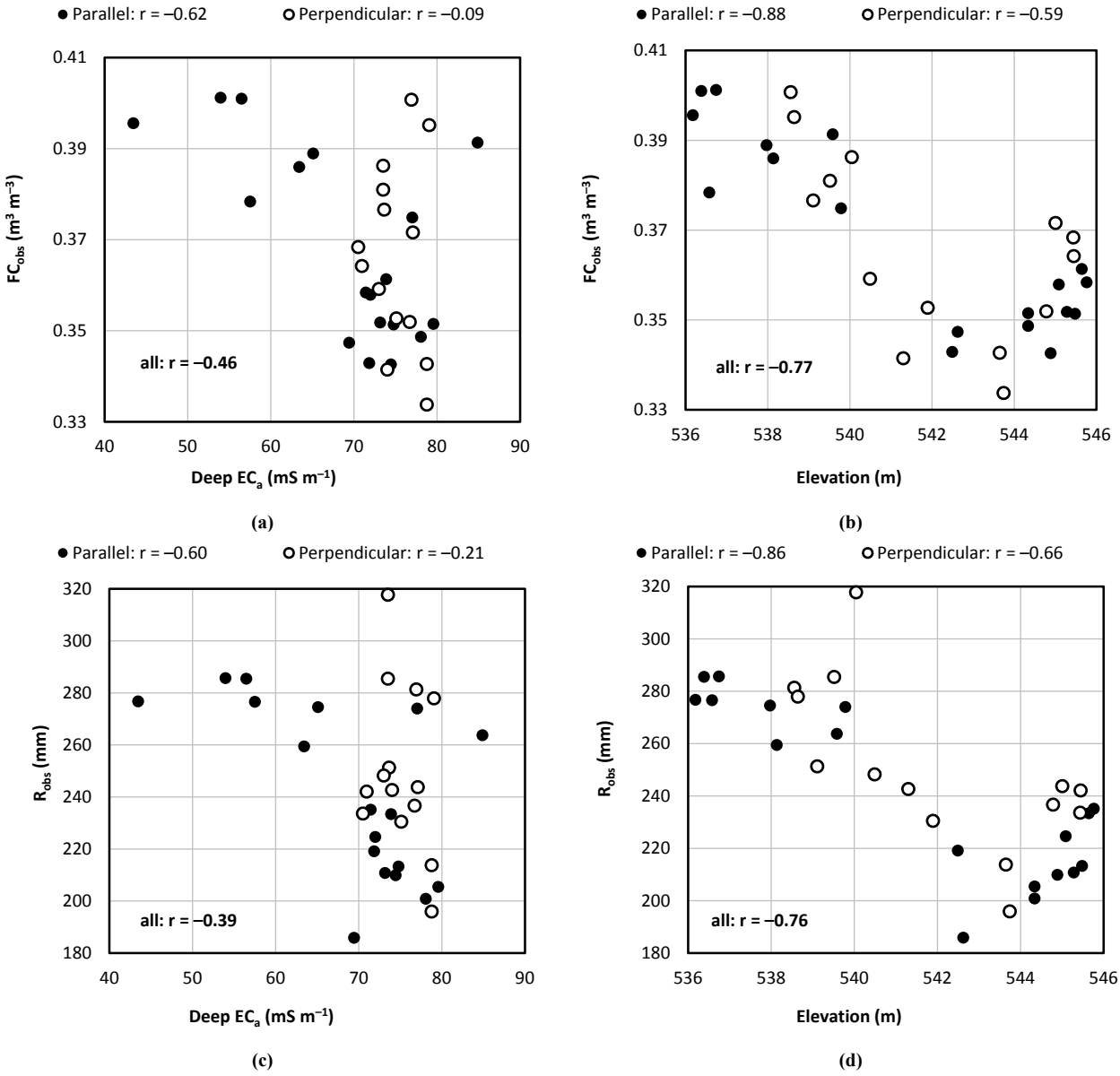

Figure 6. Average observational field capacity ($FC_{obs,a}$) and observational root zone available water capacity (R_{obs}) along parallel and perpendicular transects vs. deep apparent soil electrical conductivity (EC_a) (a and c) and elevation (b and d). Correlation coefficients (r) are for parallel and perpendicular transects.

finding was in agreement with the topographic trends in $FC_{obs,a}$ and AWC_{obs} noted in figs. 4e-f. The consistent relationship between elevation and $FC_{obs,a}$ and R_{obs} suggests that elevation might be a suitable predictor variable. The relationship between elevation and $FC_{obs,a}$, or R_{obs}, would seem to be non-causal; however, topography is important in soil formation (Jenny, 1941). Therefore, site-specific prediction of $FC_{obs,a}$ and R_{obs} based on elevation could be justified, especially for a field with marked topographic variability. Rather than being an exception unique to this field, a close relationship between topography and soil water properties has been recognized in previous research, and including elevation as an input has improved pedotransfer functions for predicting soil hydraulic properties (Leij et al., 2004). Thus, elevation *per se* is likely not the driving force for soil water property patterns, but rather topographic effects on soil formation are probably the reason for strong relationships.

PREDICTION FUNCTIONS

Our ultimate goal was to predict soil properties across the field. Predictions require a functional relationship between soil water properties and the surrogate variable. The lowest order regression equation that captured trends between $FC_{obs,a}$ and relative elevation—i.e., height above the minimum elevation—was a third-order polynomial. A fourth-order polynomial best represented the relationship between R_{obs} and the relative elevation. The polynomials satisfactorily describe the relationship between relative elevation and soil water properties (fig. 7). Overfitting was improbable with 28 and 27 degrees of freedom for $FC_{obs,a}$ and R_{obs}, respectively. Independent and dependent variables also included adequate variation to avoid clustering. The

standard error of the estimate was 0.009 m^3 m^{-3} for $FC_{obs,a}$ and 17 mm for R_{obs}. The coefficient of determination (R^2) was 0.83 (unadjusted) and 0.81 (adjusted) for the $FC_{obs,a}$ regression equation and 0.76 (unadjusted) and 0.72 (adjusted) for R_{obs}. These correlations are stronger than or comparable to regressions between EC_a and soil water properties from other research (Hezarjaribi and Sourell, 2007; Jiang et al., 2007; Hedley and Yule, 2009; Rudnick and Irmak, 2014).

Field elevations extended 0.8 m below and 1.6 m above the elevations from the measurement locations. Nine percent of the field resided below the minimum elevation of measurement locations, whereas 19% of the field was above the highest measurement location. The most prominent changes in $FC_{obs,a}$ and R_{obs} occurred where slopes were steep (figs. 4e-f). Thus, we reasoned that soil water properties for points above measured elevations were similar to properties at the highest measured elevations, and properties below the lowest measured elevation corresponded to the lowest measurement locations. Piecewise prediction functions were constructed to follow the polynomial relationships within the elevation range of the measurement locations, and represent high and low regions as described for points outside of range of measurement elevations (fig. 7). More measurements on top of the hills and in the valleys may have improved the representation of FC_{obs} and R_{obs}.

Maps of Soil Water Properties

An alternative to the field characterization approach is using gSSURGO data to produce maps of soil water properties for site-specific management. Our goal was to compare FC_a and R maps from gSSURGO (figs. 8a and 8c) to those generated from the field characterization approach (figs. 8b and 8d). Both sets of FC_a and R maps depicted similar general relationships between topography and the two soil water properties. However, the discrepancies between the two sets of maps were not merely whether FC_a and R values were classified into one of a few discrete levels by gSSRUGO or distributed throughout a continuous range by field characterization. Disagreement about the exact slope positions at which FC_a and R rapidly transitioned between high and low caused substantial differences between the two sets of soil water property maps in some parts of the field site.Overall, the $FC_{obs,a}$ map from field characterization spanned a range 26% larger than the range from gSSURGO. The R_{obs} map from field characterization spanned a range 42% larger than the range from gSSURGO. Comparing raster cell values, the root mean squared difference between gSSURGO and field characterization values was 0.031 m^3 m^{-3} for FC_a and 34 mm for R. The Nash-Sutcliffe efficiency of gSSURGO predictions versus field-characterized values gave an index of -2.08 for FC_a and -0.64 for R. This indicates that the gSSURGO map approach is not a reliable approximation of patterns derived from the field characterization method. The spatial and numerical accuracy of FC_a and R maps could be important for avoiding excessive or deficient irrigation; thus, field characterization would be recommended over gSSURGO as the source of FC_a and R maps for VRI management.

The application of FC_a and R maps extends beyond VRI. These soil water properties are associated with retention of precipitation; thus they could relate to the potential and/or severity of nitrate leaching and water and/or nitrogen stresses. Knowledge of the spatial distribution of FC and R may improve deployment of soil and plant sensors and enhance site-specific seeding and fertilization for irrigated and rainfed crops. Research and extension in applying field characterization of FC and R to advance various aspects of agronomic management could be fruitful.

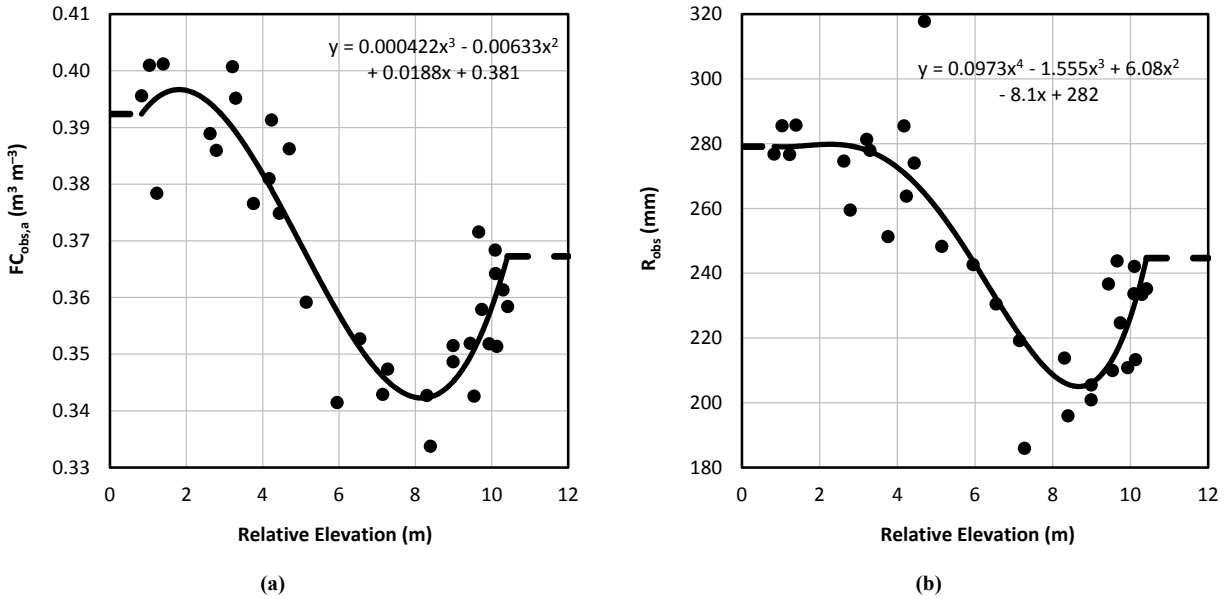

Figure 7. Piecewise prediction functions for average observational field capacity ($FC_{obs,a}$), and observational root zone available water capacity (R_{obs}) as a function of elevation above the minimum field elevation.

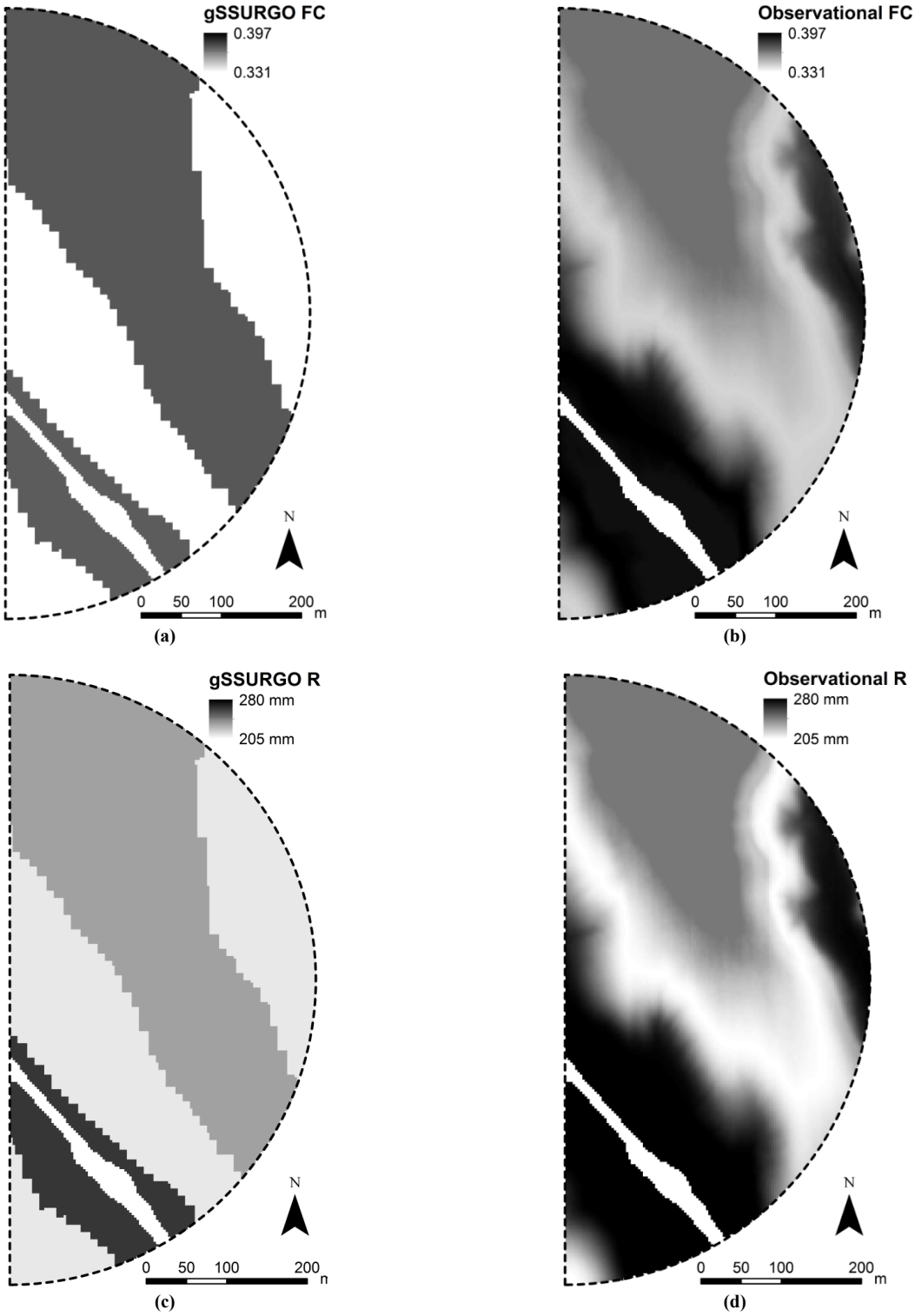

Figure 8. Maps of average field capacity (FC_a) and root zone available water capacity (R) calculated from the gridded Soil Survey Geographic database (a and c) compared to maps derived from the piecewise prediction functions (b and d).

SAMPLING SCHEMES

Success with the predictor variable approach depends on a robust sampling strategy to efficiently represent the distribution of soil water properties. As the number of sampled locations (n) increases, the observed trend in $FC_{obs,a}$ and R_{obs} should approach the true trend in $FC_{obs,a}$ and R_{obs}; therefore, the accuracy of the prediction functions should improve with an increase in the number of sampled locations. The standard error of the estimate (s) for both the $FC_{obs,a}$ and R_{obs} prediction functions—when applied to the validation set—did decrease as n increased from two to ten (fig. 9). The sampling scheme with $n = 6$ resulted in a large standard error for the R_{obs} prediction function. This was the

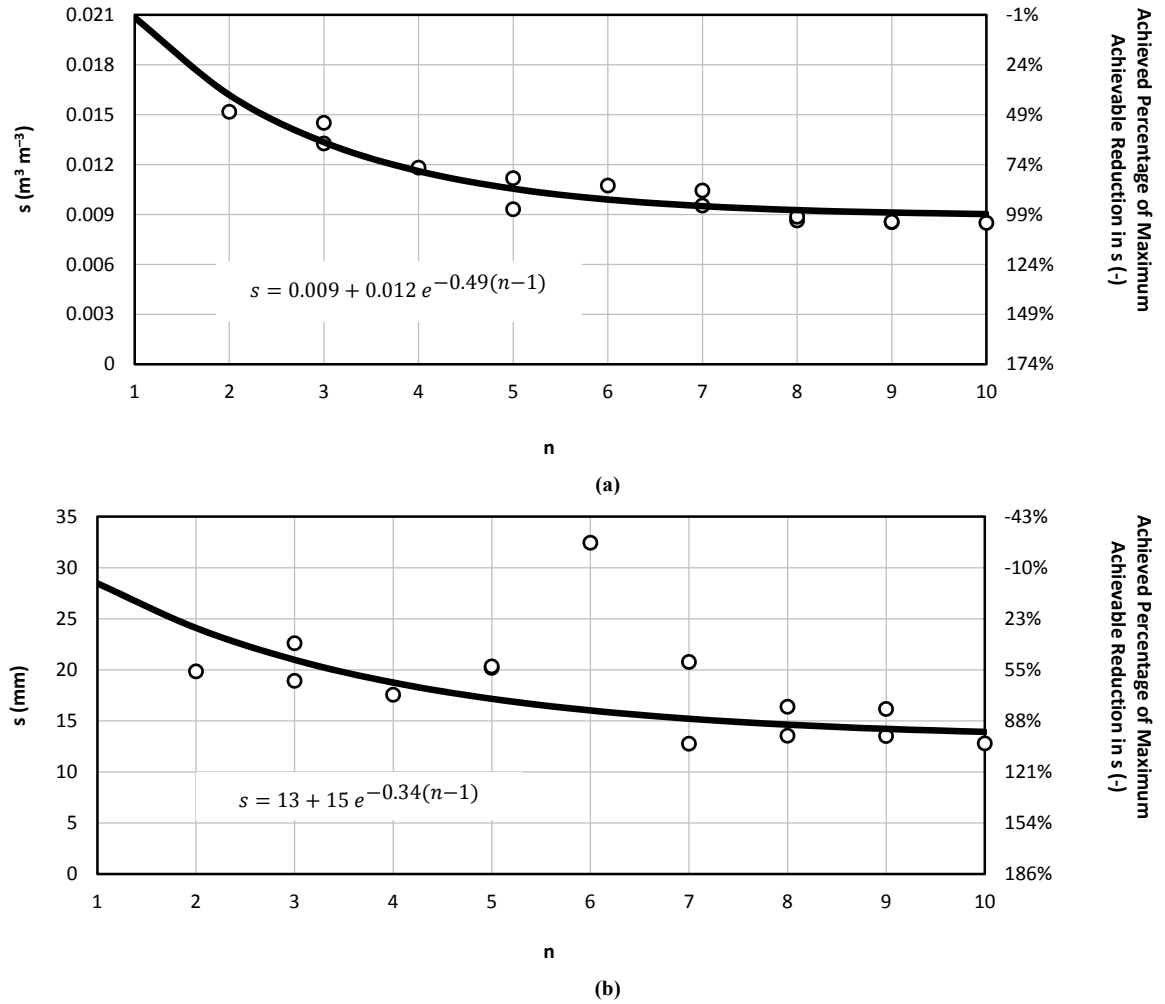

Figure 9. Decay of the standard error of the estimate (*s*) for the piecewise prediction function for average observational field capacity (a) and observational root zone available water capacity (b) with the number of sampled locations (*n*). Dots signify *s* when following a series of sampling schemes compared to data for a fixed set of 16 validation locations. Lines represent the fitted three-parameter equation.

only scheme with a small number of sampled locations that included the apparently outlying R_{obs} data point (fig. 7b). When this R_{obs} data point was included into sampling schemes with a larger number of observations its influence was dampened. These observations illustrate how outliers can affect the regression of the prediction functions—especially with a small number of sampling locations and no prior knowledge of the underlying $FC_{obs,a}$ or R_{obs} distributions. Restricting regression to lower polynomial orders can help avoid overfitting, but may limit the ability to match actual trends. Individual analysis will be required to ascertain the appropriate number of sampling locations for a specific field.

When points for the subsample were selected randomly, a portion of the elevation range of the measurement locations was often poorly characterized. Consequently, the regression equation inaccurately represented those elevations (results not shown). The sampling scheme presented here encompassed the range of elevations, which reduced the occurrence of such omissions and the ensuing errors. This finding highlighted that sampling locations should provide representative coverage throughout the entire range of the predictor variable(s).

If the irrigation management strategy requires both field capacity and available water capacity, then the number of required observations would equal the larger requirement of the two properties. The exponential decay coefficient for R_{obs} (omitting the sampling scheme with $n = 6$) was smaller than that for $FC_{obs,a}$. Thus, more sampling locations would be needed for R_{obs} than for $FC_{obs,a}$ to achieve the same reduction in *s*. According to the equations, at least 75% of the achievable reduction in *s* would be achieved at $n = 4$ for $FC_{obs,a}$ and at $n = 5$ for R_{obs}. Attaining at least 90% of the achievable reduction in *s* would require $n = 6$ for $FC_{obs,a}$ and at $n = 8$ for R_{obs}.

DISCUSSION OF EC_A

Our results showed that EC_a data were poorly correlated with soil water properties (fig. 6) or soil composition (results not shown) at our field site. Variability in fertilizer application and/or leaching was not considered to be a contributing factor for EC being a weak predictor. This differs from other research. Sudduth et al. (2005) found that EC_a related moderately or strongly to clay content and cation exchange capacity for twelve fields across the north-central United States. Rudnick and Irmak (2014) found

moderate to strong relationships between EC_a and WP and also between EC_a and volumetric water content at 33 kPa of tension for a field 30 km south of our site. The variability of EC_a and soil water properties was comparable for the two Nebraska fields. Thus, insufficient variability in EC_a and/or soil water properties is probably not the primary reason for lack of correlation between EC_a and soil water properties in our field. Differences in $FC_{obs,a}$ among measurement locations in our field do not appear to be driven by differences in soil composition within the managed root zone (results not shown). The underlying variables that cause spatial variability in $FC_{obs,a}$ at this field may be occurring below the effective measurement depth of the EC_a sensor we used or might be imperceptible using EC_a sensors. Keep in mind that our results represent the crop root zone and not individual soil cores.

Poor correlation between soil property measurements and EC_a readings was not unique to our study. Hillyer and Higgins (2014) obtained an EC_a map that exhibited "very poor correlation" with soil texture and appeared to be "not representative of observed conditions" for several fields in the northwestern United States. The cause of unacceptable results was not identified. A second EC_a measurement campaign produced data that "was deemed acceptable enough" (Hillyer and Higgins, 2014). Uniformity in R_{obs} among measurement locations with diversity in EC_a was also noted for one of two fields in Nebraska that were studied by Miller (2015). These observations suggest that the quality of EC_a data may be sensitive to when and/or how EC_a was measured (Zhu et al., 2010).

Apparent soil electrical conductivity has been shown to be a suitable predictor of soil water properties in multiple research studies which were conducted on fields containing substantial spatial disparities in soil texture within the managed root zone (Hezarjaribi and Sourell, 2007; Jiang et al., 2007; Hedley and Yule, 2009). It has been widely used and highly regarded in precision agriculture for applications including soil mapping for site-specific agricultural water management. However, our results and other studies highlight that EC_a might not be universally suitable.

SUMMARY AND CONCLUSIONS

Field characterization of field capacity (FC) and/or root zone available water capacity (R) is a procedure to map soil water properties within an individual field for site-specific water management. The first component of field characterization consists of determining average observational FC ($FC_{obs,a}$) within the managed root zone and observational R (R_{obs}) at a number of sampling locations. The $FC_{obs,a}$ can be determined from the volumetric water content of the soil profile after a thorough wetting event. The permanent wilting point can be estimated using a pedotransfer function after soil composition analysis, a pressure plate/membrane apparatus, or other laboratory procedures. The second component of field characterization consists of predicting $FC_{obs,a}$ and R_{obs} throughout the field using a surrogate or predictor variable(s). Regression relating $FC_{obs,a}$ or R_{obs} to densely measured spatial variables enables determination of the spatial distribution, and production of maps, of $FC_{obs,a}$ or R_{obs}. Field characterization of FC and R on a topographically variable field in south central Nebraska generated several recommendations for the procedure.

Instead of arbitrarily relying on the same surrogate variable for all fields, selection of predictor variables should depend on an understanding of each field and consideration of existing spatial data. Apparent soil electrical conductivity (EC_a) has proven to be useful for predicting soil water properties; however, $FC_{obs,a}$ and R_{obs} were not well-correlated to EC_a at our field site. The $FC_{obs,a}$ and R_{obs} did show a close and consistent correlation with relative elevation. Topographic attributes calculated from public DEMs, reflectance indices computed from remote sensing, and various precision agriculture products (e.g., EC_a, yield maps, grid sampling) might enhance spatial description of FC_{obs} and R_{obs}. Requirements for selecting predictor variables might be reduced if regional patterns of predictor variables (e.g. slope) could be identified.

A small number of well-chosen sampling locations may be adequate for accurate predictions when predictor variables are strongly and smoothly related to $FC_{obs,a}$ or R_{obs}. Calibration at seven locations that were distributed across the elevation range in our field resulted in $FC_{obs,a}$ and R_{obs} prediction functions that achieved 95% and 87%, respectively, of the achievable reduction in the standard error of the estimate. Sampling locations should be evenly distributed over the range of the predictor variable(s). In addition, a careful choice of regression equation is necessary to balance the risk of overfitting against the ability to simulate complex trends.

While the public soil survey may capture the general spatial trends of soil water properties, field characterization can better pinpoint the values of $FC_{obs,a}$ and R_{obs} and the transitions in these values. The public soil survey and field characterization were in agreement about the correspondence between terrain and soil water properties in our field. Nevertheless, the two sets of FC_a and R maps diverged substantially along the hillsides where sharp transitions in soil water properties occurred. The root mean squared difference between maps from the methods was 0.031 m^3 m^{-3} for FC_a and 34 mm for R. Growers and consultants must weigh the costs and benefits of field characterization as they develop data for analyzing VRI viability (Lo et al., 2016) and/or VRI management (Ritchie and Amato, 1990).

ACKNOWLEDGEMENTS

This research was supported by the Water, Energy and Agriculture Initiative from the Nebraska Corn Board, the Nebraska Soybean Board, the Agricultural Research Division at the University of Nebraska–Lincoln (UNL), and Nebraska Public Power District through the Nebraska Center for Energy Sciences Research at UNL. This work was also supported by the USDA NIFA Hatch project 1009760, the Water for Food Global Institute at the University of Nebraska, the Department of Biological Systems Engineering at UNL, and the Organization for Economic Co-operation and Development Co-operative Research Programme (contract JA00079306). The authors

are grateful to the Christenson brothers for welcoming and facilitating the use of the field site, and to Alan Boldt, Tyler Smith, and Dilshad Brar for assistance with field data collection. The authors also thank the associate editor and the reviewers for their constructive input.

APPENDIX

SOIL AND WATER TERMINOLOGY

The ASABE Standard on soil and water terminology (*ASABE Standards*, 2015) provides definitions for several terms utilized in the manuscript. Excerpts of those definitions are provided below.

- Allowable depletion: That part of soil water stored in the plant root zone managed for use by plants, usually expressed as equivalent depth of water in mm (acre-inches per acre, or inches).
- Available water capacity (AWC): The portion of soil water that can be readily absorbed by plant roots of most crops, expressed in mm water per mm soil (inches per inch, inches per foot, or total inches) for a specific soil depth. It is the amount of water stored in the soil between field capacity (FC) and permanent wilting point (WP)… Also called available water holding capacity (AWHC), or available soil water.
- Field capacity: Amount of water remaining in a soil when the downward water flow due to gravity becomes negligible…
- Full irrigation: Management of a water application to fully replace the soil water deficiency over an entire field.
- Irrigation scheduling: The process of determining when to irrigate and how much water to apply, based upon measurements or estimates of soil moisture or water used by the plant.
- Management allowed depletion: The desired soil water deficit at the time of irrigation (can be expressed as a fraction or percentage of the AWC).
- Net irrigation: The actual amount of applied irrigation water stored in the soil for plant use or moved through the soil for leaching salts.
- Permanent wilting point: Soil water content below which plants cannot readily obtain water and permanently wilt. Sometimes called "permanent wilting percentage" or WP. Often estimated as the water content corresponding to a matric potential of -1.5 MPa (-15 bar).
- Soil water deficit: Amount of water required to raise the soil water content of the crop root zone to field capacity. It is measured in mm (inches) of water. Also called soil water depletion.

REFERENCES

Allen, R. G., Pereira, L. S., Raes, D., & Smith, M. (1998). Crop evapotranspiration: Guidelines for computing crop water requirements. FAO Irrigation and Drainage Paper No. 56. Rome, Italy: United Nations FAO.

ArcGIS. (2013). ArcGIS Desktop. Ver. 10.2. Redlands, CA: ESRI.

ASABE Standards. (2015). S526.3: Soil and water terminology. St. Joseph, MI: ASABE.

Brady, R. A., Stone, L. R., Nickell, C. D., & Powers, W. L. (1974). Water conservation through proper timing of soybean irrigation. *JSWC, 29*, 266-268.

Brevik, E. C., Fenton, T. E., & Jaynes, D. B. (2003). Evaluation of the accuracy of a Central Iowa soil survey and implications for precision soil management. *Precis. Agric., 4*(3), 331-342. https://doi.org/10.1023/a:1024960708561

Daccache, A., Knox, J. W., Weatherhead, E. K., Daneshkhah, A., & Hess, T. M. (2015). Implementing precision irrigation in a humid climate: Recent experiences and on-going challenges. *Agric. Water Manag., 147*, 135-143. http://dx.doi.org/10.1016/j.agwat.2014.05.018

Deck, J. H. (2010). Hydraulic conductivity, infiltration, and runoff from no-till and tilled cropland. MS thesis. Lincoln, NE: University of Nebraska-Lincoln, Department of Biological Systems Engineering.

Evans, R. G., LaRue, J., Stone, K. C., & King, B. A. (2013). Adoption of site-specific variable rate sprinkler irrigation systems. *Irrig. Sci., 31*(4), 871-887. https://doi.org/10.1007/s00271-012-0365-x

FSA. (2014). National agricultural imagery program. Washington, DC: USDA. Retrieved from https://gdg.sc.egov.usda.gov/GDGOrder.aspx

Grimes, D. W., Yamada, H., & Dickens, W. L. (1969). Functions for cotton (*Gossypium hirsutum* L.) production from irrigation and nitrogen fertilization variables: I. Yield and evapotranspiration. *Agron. J., 61*(5), 769-773. https://doi.org/10.2134/agronj1969.00021962006100050035x

Haghverdi, A., Leib, B. G., Washington-Allen, R. A., Ayers, P. D., & Buschermohle, M. J. (2015). High-resolution prediction of soil available water content within the crop root zone. *J. Hydrol., 530*, 167-179. http://dx.doi.org/10.1016/j.jhydrol.2015.09.061

Hedley, C. B., & Yule, I. J. (2009). A method for spatial prediction of daily soil water status for precise irrigation scheduling. *Agric. Water Manag., 96*(12), 1737-1745. http://dx.doi.org/10.1016/j.agwat.2009.07.009

Hedley, C. B., Roudier, P., Yule, I. J., Ekanayake, J., & Bradbury, S. (2009). Soil water status and water table depth modelling using electromagnetic surveys for precision irrigation scheduling. *Geoderma, 199*, 22-29. http://dx.doi.org/10.1016/j.geoderma.2012.07.018

Hezarjaribi, A., & Sourell, H. (2007). Feasibility study of monitoring the total available water content using non-invasive electromagnetic induction-based and electrode-based soil electrical conductivity measurements. *Irrig. Drain., 56*(1), 53-65. https://doi.org/10.1002/ird.289

Hillyer, C. C., & Higgins, C. W. (2014). A demonstration of energy & water savings potential of variable rate irrigation. ASABE Paper No. 141914755. St. Joseph, MI: ASABE.

Jenny, H. (1941). *Factors of soil formation: A system of quantitative pedology.* New York, NY: McGraw-Hill.

Jiang, P., Anderson, S. H., Kitchen, N. R., Sudduth, K. A., & Sadler, E. J. (2007). Estimating plant-available water capacity for claypan landscapes using apparent electrical conductivity. *SSSAJ, 71*(6), 1902-1908. https://doi.org/10.2136/sssaj2007.0011

Kanwar, R. S., Baker, J. L., & Mukhtar, S. (1988). Excessive soil water effects at various stages of development on the growth and yield of corn. *Trans. ASAE, 31*(1), 133-141. https://doi.org/10.13031/2013.30678

King, B. A., Stark, J. C., & Wall, R. W. (2006). Comparison of site-specific and conventional uniform irrigation management for potatoes. *Appl. Eng. Agric., 22*(5), 677-688. https://doi.org/10.13031/2013.22000

Kitchen, N. R., Sudduth, K. A., Myers, D. B., Drummond, S. T., & Hong, S. Y. (2005). Delineating productivity zones on claypan soil fields using apparent soil electrical conductivity. *Comput. Electron. Agric., 46*(1), 285-308. http://dx.doi.org/10.1016/j.compag.2004.11.012

Kranz, W. L., Evans, R. G., Lamm, F. R., O'Shaughnessy, S. A., & Peters, R. T. (2012). A review of mechanical move sprinkler irrigation control and automation technologies. *Appl. Eng. Agric., 28*(3), 389-397. https://doi.org/10.13031/2013.41494

Leij, F. J., Romano, N., Palladino, M., Schaap, M. G., & Coppola, A. (2004). Topographical attributes to predict soil hydraulic properties along a hillslope transect. *Water Resour. Res., 40*(2), W02407. https://doi.org/10.1029/2002WR001641

Lo, T., Heeren. D., M., Martin. D., L., Mateos, L., Luck, J. D., & Eisenhauer, D. E. (2016). Pumpage reduction by using variable-rate irrigation to mine undepleted soil water. *Trans. ASABE, 59*(5), 1285-1298. https://doi.org/10.13031/trans.59.11773

Martin, D. L., Stegman, E. C., & Fereres, E. (1990). Irrigation scheduling principles. In G. J. Hoffman, T. A. Howell, & K. H. Solomon (Eds.), *Management of farm irrigation systems* (pp. 155-203). St. Joseph, MI: ASAE.

Matthews, M. A., & Anderson, M. M. (1988). Fruit ripening in *Vitis vinifera* L.: Responses to seasonal water deficits. *American J. Enol. Viticulture, 39*(4), 313-320.

McCarthy, A. C., Hancock, N. H., & Raine, S. R. (2014). Development and simulation of sensor-based irrigation control strategies for cotton using the VARIwise simulation framework. *Comput. Electron. Agric., 101*, 148-162. http://dx.doi.org/10.1016/j.compag.2013.12.014

Merriam, J. L. (1966). A management control concept for determining the economical depth and frequency of irrigation. *Trans. ASAE, 9*(4), 492-498. https://doi.org/10.13031/2013.40014

Microsoft Excel. (2010). Microsoft Excel 2010. Redmond, WA: Microsoft.

Miller, K. A. (2015). Estimating potential water savings based on soil water content, geospatial data layers, and VRI pivot control resolution. MS thesis. Lincoln: University of Nebraska-Lincoln, Department of Biological Systems Engineering.

Mortensen, I. I. (2011). Intraseasonal management strategies for deficit irrigation. MS thesis. Lincoln: University of Nebraska-Lincoln, Department of Biological Systems Engineering.

NCEI. (2017). Climate data online: Daily summaries. Asheville, NC: NOAA. Retrieved from https://www.ncdc.noaa.gov/cdo-web/datasets/GHCND/stations/GHCND:US10hami002/detail

NDNR. (2017). Nebraska rainfall assessment and information network. Lincoln: Nebraska Department of Natural Resources. Retrieved from http://nerain.dnr.ne.gov/NeRAIN/Reports/PrecipDaily.asp?Group=Station&Item=141&StaName=hami004

NRCS. (2015). Gridded soil survey geographic (gSSURGO) by state. Washington, DC: Natural Resources Conservation Service. Retrieved from https://gdg.sc.egov.usda.gov/GDGOrder.aspx

O'Shaughnessy, S. A., Evett, S. A., Andrade, A., Workneh, F., Price, J. A., & Rush, C. M. (2016). Site-specific variable-rate irrigation as a means to enhance water use efficiency. *Trans. ASABE, 59*(1), 239-249. https://doi.org/10.13031/trans.59.11165

Rhoades, J. D., Manteghi, N. A., Shouse, P. J., & Alves, W. J. (1989). Soil electrical conductivity and soil salinity: New formulations and calibrations. *SSSAJ, 53*(2), 433-439. https://doi.org/10.2136/sssaj1989.03615995005300020020x

Ritchie, J. T., & Amato, M. (1990). Field evaluation of plant extractable soil water for irrigation scheduling. *Acta Hortic., 278*, 595-616. https://doi.org/10.17660/ActaHortic.1990.278.59

Romano, N., & Santini, A. (2002). Field. In J. H. Dane, & C. Topp. G. (Eds.), *Methods of soil analysis: Part 4 physical methods* (pp. 721-738). Madison, WI: SSSA. https://doi.org/10.2136/sssabookser5.4.c26

Rudnick, D. R., & Irmak, S. (2014). Implementation of a soil water extraction model on a spatial domain using field capacity and apparent electrical conductivity relationships. *Trans. ASABE, 57*(5), 1359-1373. https://doi.org/10.13031/trans.57.10515

Sadler, E. J., Evans, R. G., Buchleiter, G. W., King, B. A., & Camp, C. R. (2000). Design considerations for site specific irrigation. *Proc. 4th Decennial Natl. Irrig. Symp.* (pp. 304-315). St. Joseph, MI: ASAE.

Sadler, E. J., Evans, R. G., Stone, K. C., & Camp, C. R. (2005). Opportunities for conservation with precision irrigation. *JSWC, 60*(6), 371-378.

Sadras, V. O., & Milroy, S. P. (1996). Soil-water thresholds for the responses of leaf expansion and gas exchange: A review. *Field Crops Res., 47*(2), 253-266. http://dx.doi.org/10.1016/0378-4290(96)00014-7

Saxton, K. E., & Rawls, W. J. (2006). Soil water characteristic estimates by texture and organic matter for hydrologic solutions. *SSSAJ, 70*(5), 1569-1578. https://doi.org/10.2136/sssaj2005.0117

Simley, J. D., & Carswell Jr., W. J. (2009). The national map: Hydrography. Fact Sheet 2009-3054. Rolla, MO: USGS. Retrieved from http://pubs.usgs.gov/fs/2009/3054/pdf/FS2009-3054.pdf

Steduto, P., Hsiao, T. C., Raes, D., & Fereres, E. (2009). Aquacrop: The FAO crop model to simulate yield response to water: I. Concepts and underlying principles. *Agron. J., 101*(3), 426-437. https://doi.org/10.2134/agronj2008.0139s

Stone, K. C., Bauer, P. J., & Sigua, G. C. (2016). Irrigation management using an expert system, soil water potentials, and vegetative indices for spatial applications. *Trans. ASABE, 59*(3), 941-948. https://doi.org/10.13031/trans.59.11550

Sudduth, K. A., Kitchen, N. R., Wiebold, W. J., Batchelor, W. D., Bollero, G. A., Bullock, D. G., Thelen, K. D. (2005). Relating apparent electrical conductivity to soil properties across the north-central USA. *Comput. Electron. Agric., 46*(1), 263-283. http://dx.doi.org/10.1016/j.compag.2004.11.010

UNL Extension. (2014). Nutrient management for agronomic crops. EC155. T. M. Shaver (Ed.). Lincoln: University of Nebraska-Lincoln.

USGS. (2014). 1/9 arc-second National Elevation Dataset. Reston, VA: USGS. Retrieved from https://gdg.sc.egov.usda.gov/GDGOrder.aspx

Zhu, Q., Lin, H., & Doolittle, J. (2010). Repeated electromagnetic induction surveys for improved soil mapping in an agricultural landscape. *SSSAJ, 74*(5), 1763-1774. https://doi.org/10.2136/sssaj2010.0056